JOURNAL OF SPACECRAFT AND ROCKETS
Vol. 38, No. 2, March–April 2001

Turbulent Boundary Layers with Foreign Gas Transpiration

Jens Meinert* and Jörg Huhn†
Dresden University of Technology, D-01062 Dresden, Germany
and
Erhan Serbest‡ and Oskar J. Haidn§
DLR, German Aerospace Research Center, D-74239 Lampoldshausen, Germany

Blowing through the wall is one of the most efficient methods to influence the characteristics of a turbulent boundary layer such as heat transfer, skin friction, boundary-layer profiles, and flow separation. The most important technical application is to cool a permeable wall with a coolant mass flow through the wall, known as transpiration cooling. Designing transpiration-cooled devices requires the knowledge of empirical correlations for the calculation of skin friction and heat transfer in the case of blowing. The results of velocity and temperature boundary-layer profile measurements made at the Dresden University of Technology were used to characterize the influence of foreign gas transpiration on skin friction and heat transfer. Simple empirical correlations describing skin friction and heat transfer reduction as functions of the blowing ratio and especially the blowing gas properties were found. Further investigations deal with flow separation due to blowing, and a universal critical blowing parameter is defined. The empirical correlations have also been verified by means of a numerical calculating procedure. Measurements made at the German Aerospace Center in Lampoldshausen using an H_2/O_2 combustion chamber delivered experimental heat transfer results in the case of hot gas parameters according to practical applications.

Nomenclature

c_f	=	skin-friction coefficient
c_p	=	specific heat capacity, J/(kg · K)
D_F	=	damping factor
d	=	diameter, m
F	=	blowing ratio
$k^{*,**}_{M,T,c_p}$	=	correcting factors
M	=	molecular weight, kg/kmol
$\dot{m}$	=	mass flow, kg/s
$Pr_{(t)}$	=	(turbulent) Prandtl number
p	=	pressure, Pa
$\hat{q}$	=	heat flux density, W/m^2
R	=	gas constant, J/(kg · K)
Re	=	Reynolds number
Sc_t	=	turbulent Schmidt number, 0.8
St	=	Stanton number
$T_{(\tau)}$	=	Kelvin (friction) temperature, K
$u_{(\tau)}$	=	main (friction) velocity, m/s
v	=	velocity in y direction, m/s
x, y	=	streamwise, perpendicular coordinate, m
δ	=	boundary-layer thickness, m
η	=	dynamic viscosity, Pa · s
κ	=	isentropic exponent
κ_m	=	von Kármán constant for momentum transport, 0.41
κ_t	=	von Kármán constant for energy transport, 0.47
λ	=	heat conductivity, W/(m · K)
ξ	=	mass fraction, kg/kg
ρ	=	density, kg/m^3
τ	=	shear stress, N/m^2

Subscripts and Superscripts

aw	=	adiabatic wall condition
c	=	coolant
w	=	hot-gas side wall
0	=	reference without transpiration
∞	=	static main flow condition
$+$	=	Prandtl coordinates

Introduction

THERE are several possibilities to realize turbulent boundary layers with mass transport from the wall into the flow. Blowing mass through holes, slits, or a porous wall is conceivable, as well as evaporation of the outer wall layer (ablation cooling). In the case of coolant transport through a slit or a line of holes (different angles of injection possible), the procedure is called film cooling. The effusion cooling involves blowing through a large number of holes, which are uniformly distributed in the wall, whereas the cooling of a permeable wall (for instance, made of sintered material or fiber ceramics) is called transpiration cooling.

The most efficient method of cooling a thermally stressed wall is transpiration cooling. This is due to two special effects: 1) the intensive heat transfer inside the wall due to the very large inner surface and 2) the decrease of heat transfer in the hot-gas boundary layer due to the blowing of coolant at the wall. Numerous practical applications are imaginable for this kind of boundary-layer modification: decrease of skin friction on the surface of high speed or reentry vehicles and reduction of heat transfer to the wall in hot-gas flows of rocket nozzles or gas turbine combustion chambers. The most important factors are 1) the coolant mass flow density $\rho_w v_w$ described by the blowing ratio $F = \rho_w v_w/(\rho_\infty u_\infty)$, 2) the properties of coolant and hot gas (main flow) expressed in terms of the molecular weights M_c and M_∞, 3) the ratio between the wall temperature T_w and the static hot-gas temperature T_∞ or the adiabatic wall temperature T_{aw}, respectively, and 4) the flow and geometrical conditions described by the Reynolds number related to the streamwise coordinate Re_x (plate) or to the local diameter Re_d (tube or nozzle).

For the construction of a thermally high stressed flow component, the skin-friction and heat transfer conditions have to be such that destruction of the wall due to overheating does not occur. Using a transpiration-cooled system, it is possible to achieve an effective

Received 9 June 2000; presented as Paper 2000-3386 at the 36th Joint Propulsion Conference, Huntsville, AL, 17–19 July 2000; revision received 11 December 2000; accepted for publication 15 December 2000.

*Scientific Assistant, Institute of Thermodynamics, Department of Mechanical Engineering.
†Professor, Institute of Thermodynamics, Department of Mechanical Engineering.
‡Research Engineer, Department of Technology.
§Head, Department of Technology. Member AIAA.

decrease in wall shear stress and heat flux density to the wall. For this reason the component designer has to calculate the friction and heat transfer conditions considering all effects of interest. The present paper will introduce simple empirical equations to take into account the impact of transpiration on a turbulent boundary layer, especially with respect to the transpiration mass flow and the coolant properties, respectively. The predicted correlations are based on the analysis of detailed measurements using a special hot-air test facility at the Dresden University of Technology. The paper will describe the measurements as well as the data evaluation procedures to show the accuracy of experimental investigations; the results will be verified using a numerical solution of the boundary-layer balance equations. Heat transfer measurements using a H_2/O_2 model combustion chamber at the German Aerospace Research Center in Lampoldshausen yield several experimental results according to practical test conditions and show an agreement with the predicted correlations. The designer of a transpiration-cooled system first has to calculate the skin-friction and heat transfer coefficients assuming an impermeable wall (unblown case) using empirical equations valid for the specific application. The second step is to consider the effect of transpiration (coolant mass flow density and properties, temperature ratio) utilizing the present simple correlations to determine corrected skin-friction and heat transfer coefficients.

To predict the influence of transpiration on the friction characteristics (wall shear stress τ_w), the skin-friction parameter

$$c_f/2 = \tau_w \big/ \rho_\infty u_\infty^2 \tag{1}$$

is used. Heat transfer is determined defining the Stanton number

$$St = \frac{\hat{\dot{q}}_w}{\rho_\infty u_\infty c_{p\infty}(T_{\mathrm{aw}} - T_w)} \tag{2}$$

including the heat flux density at the wall $\hat{\dot{q}}_w$ due to convection. Typically the adiabatic wall temperature (recovery factor valid for turbulent flat plate boundary layer)

$$T_{\mathrm{aw}} = T_\infty + \sqrt[3]{Pr_\infty}\left(u_\infty^2 \big/ 2c_{p\infty}\right) \tag{3}$$

is employed as the hot-gas reference temperature with respect to convective heat transfer in the case of high-speed flow. To eliminate the influences of geometry and flow characteristics, it is recommendable to use the relation of blown and unblown conditions c_f/c_{f0} and St/St_0. For the calculation of the skin-friction coefficient $c_{f0}/2$ and the Stanton number St_0 without transpiration, it is necessary to consider temperature conditions that are similar to those present in the blown case because of their temperature dependence (especially the blown wall temperature T_w).

Numerous publications on heat and mass transfer problems in turbulent boundary layers are available in the field of experimental investigations[1–6] and theoretical procedures[7–11] using identical or foreign injectants. Most of these papers deal with heat transfer measurements, especially in high-speed flows ($Ma_\infty \geq 3$), to predict the convective heat flux density from the thermal energy balance at the wall.[1–4] There is only a small number of skin-friction measurements,[5] particularly in the case of foreign gas injection. A survey of several works[6] shows large differences with respect to the experimental results achieved, as well as the suggested empirical correlations. The theoretical handling of a turbulent boundary layer with foreign gas injection requires the solution of mass, momentum, thermal energy, and species balance equations. When simplifying assumptions (one- or two-dimensional coordinates, mixing length turbulence model) are introduced, analytical[7,8] and numerical solutions[9] are given in the literature. Several works[10,11] deal with approximating solutions of the momentum and energy balance to determine the temperature ratio $(T_w - T_c)/(T_\infty - T_c)$ depending on different factors. The motivation after analyzing numerous publications was to create a closed set of simple engineering equations to describe all effects of interest referring to foreign gas transpiration.

Table 1 Parameter of measuring section

Parameter	Specification
Cross section	Height × width = 100×114 mm^2
Static temperature	$25 \leq t_\infty \leq 300$°C (variable)
Hot-gas flow	$u_\infty \leq 160$ m/s; $Ma_\infty \leq 0.35$; $3 \times 10^5 \leq Re_x \leq 3 \times 10^6$
Streamwise length	$x_{\mathrm{total}} = 470$ mm; $200 \leq x_{\mathrm{porous}} \leq 470$ mm
Porous wall	Sintered stainless steel, porosity approximately 30%
Coolant gases	Air, N_2, He, or Ar; $\dot{V}_c \leq 1100$ standard liter (N_2)/min

Boundary-Layer Investigations

Hot-Gas Test Facility at Dresden University of Technology

For detailed experimental investigation of a turbulent, flat plate boundary layer with transpiration of different gases, a hot-air wind tunnel was built at the Institute of Thermodynamics. The air is supplied by a blower ($\dot{V}_{\max} \approx 5000$ m^3/h) and heated using a heat exchanger (260 kW) and an electrical heater (100 kW). Figure 1 shows the schematic configuration of the test facility. The measuring section consists of a nearly square flow channel, and a porous wall made of sintered stainless steel is installed in the bottom of the channel. Table 1 gives some general information on geometrical, flow, and temperature parameters of this test facility.

Hot-gas velocity and temperature are infinitely variable; the maximum velocity is measured according to a maximum hot-gas temperature. At the entrance of the measuring section, the existing boundary layer is sucked, a new boundary layer develops at the bottom of the channel, and transition to a fully turbulent flow is initiated by means of a trip wire. Preliminary measurements of velocity profiles (hot-wire probe) and streamwise wall shear stress distributions (Preston probe) without blowing yield an excellent agreement with the turbulent flat plate boundary-layer characteristics (thickness $5 \leq \delta \leq 12$ mm). The coolant gases are supplied from gas bottles and flow into the coolant reservoir below the porous wall. Figure 1 also shows details of the measuring section including probe support, coolant supply, and pyrometer.

Measuring Equipment

To predict skin friction and heat transfer from boundary-layer profiles, the following measurements are required: 1) boundary-layer velocity profiles $u(y)$, 2) local static pressure $p_\infty \neq f(y)$, 3) boundary-layer temperature profiles $t(y)$, 4) wall temperature of the porous surface $t_w(x)$, and 5) coolant mass flow density at the wall $\rho_w v_w$. To measure the boundary-layer velocity and temperature distribution, a combined sensor containing a static pressure probe, a pitot probe, and a miniature thermocouple is used. The static pressure probe consists of a small pipe with holes along the side (hole diameter 0.2 mm), the pitot probe has a fish mouth profile (height × width = 0.25×2.5 mm^2), and the temperature probe consists of a special NiCr/Ni thermocouple (wire diameter 70 μm). This combined probe can be moved perpendicular to the wall as well as in the streamwise direction ($\Delta x_{\min} = \Delta y_{\min} = 6.25$ μm) to enable boundary-layer profile measurements in the middle of the channel along the entire length at the porous wall.

To prevent a disturbance of the coolant mass flow and therewith the surface temperature field, a contactless temperature measuring procedure was chosen. An infrared pyrometer (spectral range 8–11 μm) is used, which takes measurements through special windows on the top of the channel. After calibration of the pyrometer ($\Delta t_w = \pm 2$ K), surface temperatures are measurable in the range of $25 \leq t_w \leq 300$°C (pyrometer also mobile). Two mass flow controllers determine the coolant mass flow supplied from gas bottles (He, Ar, or N_2) or an air compressor (measurement of $\dot{V}_c$, calculation of $\rho_w v_w$ assuming ideal gas behavior).

Data Evaluation

There are different problems during the evaluation of measured data, especially in the case of foreign gas transpiration due to the strong density variation. The main problems are the prediction of the density distribution without the possibility of gas composition measurement and the development of laws of the wall valid for compressible boundary layers (temperature as well as composition dependence) considering mass transfer at the wall. To calculate

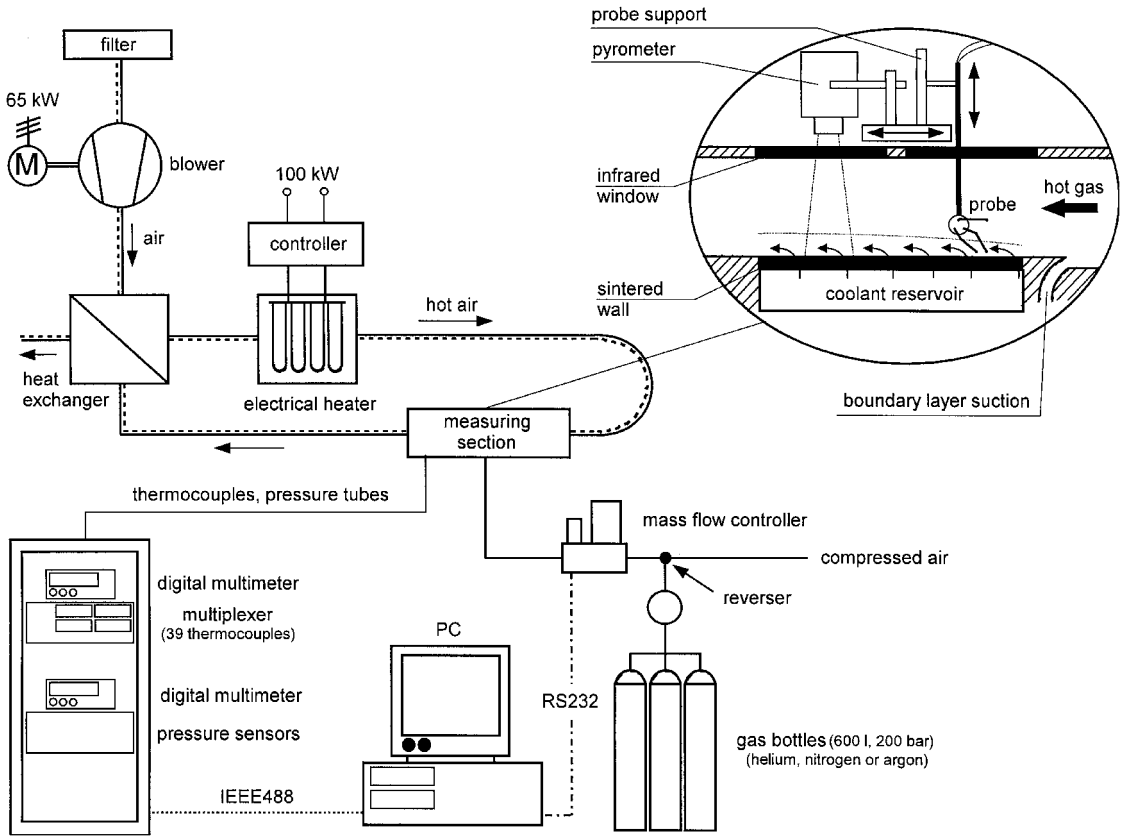

Fig. 1 Schematic of hot air test facility at Dresden University of Technology.

velocity profiles from measured dynamic pressure p_{dyn}, it is necessary to know the local density distribution $\rho(y)$ as a function of the temperature $t(y)$ and the foreign gas mass fraction $\xi_c(y)$. A special equation to predict the velocity from the dynamic pressure assuming ideal gas conditions is given for subsonic flow by

$$u = \sqrt{\frac{2\kappa}{\kappa - 1} R_m T \left[\left(\frac{p_{\mathrm{dyn}}}{p_\infty} + 1 \right)^{(\kappa - 1)/\kappa} - 1 \right]} \tag{4}$$

The variable R_m describes the apparent gas constant of the binary gas mixture defined as $R_m = \xi_c R_c + (1 - \xi_c) R_\infty$. To predict R_m, the concentration profile was determined using the analogy of momentum transport and diffusion in a turbulent boundary layer. When the one-dimensional momentum and diffusion balance is integrated once, the resulting equations are divided, and $Sc_t = \text{const}$ and $\xi_c(y \to \delta) = 0$ (at the edge of the boundary layer) are assumed, the correlation of mass fraction and velocity

$$\xi_c(y) = 1 - \left\{ \left[\frac{2F}{c_f} \frac{u(y)}{u_\infty} + 1 \right] \Big/ \left[\frac{2F}{c_f} + 1 \right] \right\}^{Sc_t} \tag{5}$$

is obtained. A simplification of Eq. (5) is possible assuming $Sc_t = 1$:

$$\xi_c = \xi_{cw}(1 - u/u_\infty) \quad \text{with} \quad \xi_{cw} = 1 - (2F/c_f + 1)^{-Sc_t} \tag{6}$$

The determination of the wall shear stress τ_w and the convective heat flux density $\hat{q}_w$ from boundary-layer profiles is possible using the so-called Clauser method. This procedure is based on the comparison of measured velocity or temperature profiles with theoretical laws of the wall $u^+(y^+)$ or $t^+(y^+)$ valid for the present boundary-layer configuration. When the free parameters $c_f/2$ or $\hat{q}_w$ are varied, the difference between theory and experiment can be minimized. When the (wall) friction velocity and friction temperature

$$u_\tau = \sqrt{\frac{\tau_w}{\rho_w}} = u_\infty \sqrt{\frac{c_f}{2} \frac{\rho_\infty}{\rho_w}}$$

$$T_\tau = \frac{|\hat{q}_w|}{\rho_w c_{pw} u_\tau} = St \sqrt{\frac{2}{c_f}} \sqrt{\frac{\rho_\infty}{\rho_w}} \frac{c_{p\infty}}{c_{pw}} |T_w - T_{\mathrm{aw}}| \tag{7}$$

are defined, the measured data can be converted into so-called dimensionless Prandtl coordinates

$$u^+ = u/u_\tau, \qquad t^+ = (t - t_w)/T_\tau$$

$$y^+ = \rho y u_\tau / \eta, \qquad v_w^+ = v_w/u_\tau \tag{8}$$

with the definition of y^+ using local values of density and viscosity in opposition to other publications defining $\tilde{y}^+ = \rho_w y u_\tau / \eta_w$. The consideration of the density (ρ_∞/ρ_w) and heat capacity ratios $(c_{p\infty}/c_{pw})$ in Eq. (7) is important because τ_w and $\hat{q}_w$ are related to wall conditions in contrast to $c_f/2$ and Stanton number St [related to the freestream condition, see also Eqs. (1) and (2)]. The density at the wall ρ_w is calculated as a function of t_w and ξ_{cw} assuming an ideal gas and using Eq. (6) (additional coolant exit velocity v_w and v_w^+ can be predicted from measured coolant mass flow density $\rho_w v_w$).

Figure 2 shows measured velocity profiles presented in Prandtl coordinates (symbols) compared with a compressible law of the wall (lines) and an incompressible law (broken line). The compressible law will be developed in the following; the incompressible law with blowing is taken from Stevenson.[12] Varying wall shear stress τ_w results in a parallel displacement of the calculated values. The τ_w value that gives the best agreement represents the local wall shear stress.

To develop a universal law of the wall for turbulent, flat plate boundary layers considering blowing and compressibility, the one-dimensional momentum balance equation

$$\rho_w v_w \frac{\mathrm{d}u}{\mathrm{d}y} = \frac{\mathrm{d}}{\mathrm{d}y} \left(\eta_{\mathrm{eff}} \frac{\mathrm{d}u}{\mathrm{d}y} \right) \tag{9}$$

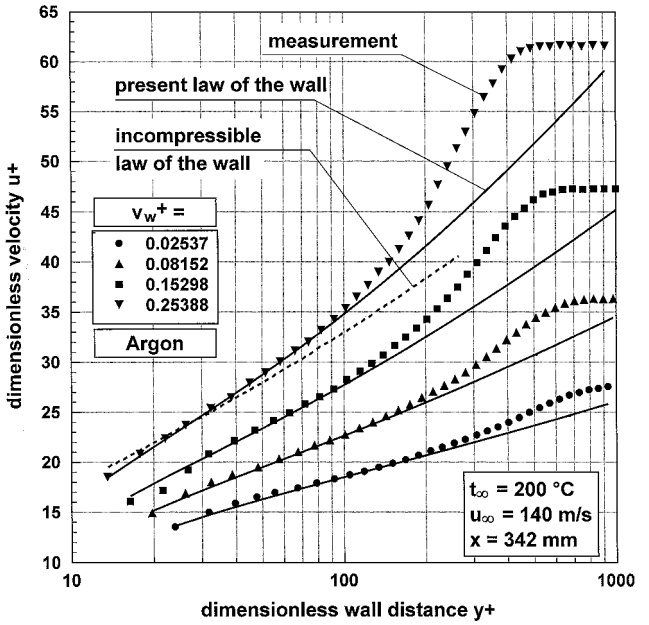

Fig. 2 Comparison of measured and theoretical velocity distributions.

has to be used (including mass balance). The subsequent steps are to integrate Eq. (9) once, to introduce the boundary conditions and Prandtl coordinates and to substitute the effective viscosity η_{eff} (sum of the molecular and turbulent part) by means of van Driest's mixing length hypothesis. The following equation is the result:

$$v_w^+ u^+ + 1 = \frac{\rho}{\rho_w}\left(1 + \kappa_m^2 y^{+2} D_F^2 \frac{du^+}{dy^+}\right)\frac{du^+}{dy^+} \tag{10}$$

The (positive) solution of the ordinary quadratic equation (10) is given by

$$\frac{du^+}{dy^+} = \frac{2(\rho_w/\rho)\left(1 + v_w^+ u^+\right)}{1 + \sqrt{1 + 4\kappa_m^2 y^{+2} D_F^2 (\rho_w/\rho)\left(1 + v_w^+ u^+\right)}} \tag{11}$$

The original van Driest damping factor D_F has to be modified for consideration of foreign gas injection at the wall based on a suggestion by Patankar and Spalding (see Landis[9]) considering the momentum balance equation (9):

$$D_F = 1 - \exp\left[\frac{y^+}{A^+}\frac{\sqrt{\tau/\rho}}{\sqrt{\tau_w/\rho_w}}\right]$$

$$= 1 - \exp\left[-\frac{y^+}{A^+}\sqrt{\frac{\rho_w}{\rho}\left(1 + v_w^+ u^+\right)}\right] \tag{12}$$

with $A^+ \approx 26$. The density relation ρ_w/ρ is different from unity (compressible) and defined with respect to the temperature and gas composition dependence as

$$\frac{\rho_w}{\rho} = \frac{T}{T_w}\frac{M_c + (M_\infty - M_c)\left(1 - u^+/u_\infty^+\right)\xi_{cw}}{M_c + (M_\infty - M_c)\xi_{cw}} \tag{13}$$

with ξ_{cw} taken from Eq. (6). Equations (11–13) permit the numerically calculation of the velocity profile $u^+(y^+)$ (Runge–Kutta procedure) beginning at the wall ($y^+ = 0$ and $u^+ = 0$). This special law of the wall is only valid in the logarithmic region of the profile because of the lack of consideration of any wake function. In comparison to the incompressible law (broken line gives only one point of intersection), the derived compressible law shows excellent agreement with the measured velocity distributions in the nonisothermal case of argon injection (see results in Fig. 2).

To predict the convective heat flux density $\hat{\dot{q}}_w$ from experimental temperature profiles $t^+(y^+)$, a compressible temperature law is needed. Performing similar steps starting with the one-dimensional thermal energy balance (neglecting kinetic energy term) and introducing a mixing length hypothesis to describe the effective heat conductivity λ_{eff} results in

$$\frac{dt^+}{dy^+} = \left[\frac{\rho_w}{\rho c_p}\left(c_p^{\text{av}} v_w^+ t^+ + c_{pw}\right)\right] \Big/ \left(\frac{1}{Pr} + \kappa_m \kappa_t y^{+2} D_F^2 \frac{du^+}{dy^+}\right)$$

$$\text{with} \quad c_p^{\text{av}} = \int_0^y c_p(\xi_c)\, dy \approx \frac{c_p + c_{pw}}{2} \tag{14}$$

The local heat capacity is defined as $c_p = \xi_c c_{pc} + (1 - \xi_c) c_{p\infty}$ neglecting the small temperature dependence of $c_{p\infty}$ (air). By the use of Eqs. (12) and (13), the numerical calculation of temperature profile $t^+(y^+)$ beginning at the wall ($y^+ = 0$ and $t^+ = 0$) is possible. During this procedure, the dependence of binary gas mixture properties has to be taken into account, especially the nonlinear dependence of the Prandtl number $Pr(\xi_c)$ in the case of a helium–air mixture. A detailed development of the introduced equations (data evaluation and laws of the wall) and a description of the test facility and preliminary investigations containing all necessary information are given in a work by Meinert.[13]

Experimental Results

Prediction of Reference Data

The determination of reference skin-friction coefficients $c_{f0}/2$ and heat transfer data St_0 without blowing was carried out by comparing measured profiles for the nonblowing case with correlating laws of the wall, which yields two correlations valid for this specific test facility, $c_{f0}/2$ or $St_0 = f[Re_x^{-0.2}, (T_{\text{aw}}/T_w)^n]$. To calculate $c_{f0}/2$ or Stanton number St_0, similar temperature conditions have to be used (temperature correction), especially the wall temperature T_w for the blowing case.

Decrease of Skin Friction

As is known from the literature, the decrease of the skin-friction coefficient depends on the blowing rate F, the hot-gas and coolant properties, and the temperature ratio T_{aw}/T_w, respectively. An additional influence of Mach number Ma_∞ is noted from several publications, but could not verified during these investigations because of test facility limits. An empirical correlation to describe the blowing rate dependence of c_f/c_{f0} can be derived from the momentum balance as shown.[14] Adding two universal correction factors k_M and k_T (in the original $k_M = k_T = 1$) yields the following equation:

$$\frac{c_f}{c_{f0}} = \left(\frac{2F}{c_{f0}} k_M k_T\right) \Big/ \left[\exp\left(\frac{2F}{c_{f0}} k_M k_T\right) - 1\right] \tag{15}$$

The introduction of a modified blowing ratio $2F/c_{f0}$ leads to the elimination of geometrical and flow influences; with increasing blowing ratio an exponential decrease in skin friction can be stated. An investigation of the coolant property effect on the skin friction shows a strong influence. Figure 3 shows experimental skin-friction data for an isothermal boundary layer using different transpiring gases: helium, air, argon, or freon-12 (CCl_2F_2, taken from Romanenko and Kharchenko[5]). The experimental results show an increasing effect on the skin friction with decreasing molecular weight of the blowing gas. The curves in Fig. 3 represent Eq. (15) under isothermal conditions ($k_T = 1.0$) after defining a new property correction factor based on the molecular weight ratio $k_M = (M_\infty/M_c)^{0.8}$. The molecular weight correction was selected because of the nonapplicability of a viscosity correction.

With respect to the ideal gas equation, the molecular weight ratio is proportional to the density ratio ($t = \text{const} \rightarrow M_\infty/M_c \sim \rho_\infty/\rho_c$), and thus, a physical background is recognizable. In the case of a nonisothermal boundary layer, an additional influence of the temperature ratio T_{aw}/T_w is detectable. The present measurements are in very good agreement with a temperature correction factor of $k_T = (T_{\text{aw}}/T_w)^{0.8}$; however, the verified temperature range was only up to $T_{\text{aw}}/T_w \approx 1.5$ because of the test facility limits. The use of this k_T definition at higher ratios (rocket thrust chambers up to $T_{\text{aw}}/T_w \approx 7.0$) is not recommended. A more reasonable suggestion seems to be the use of temperature correction according to the

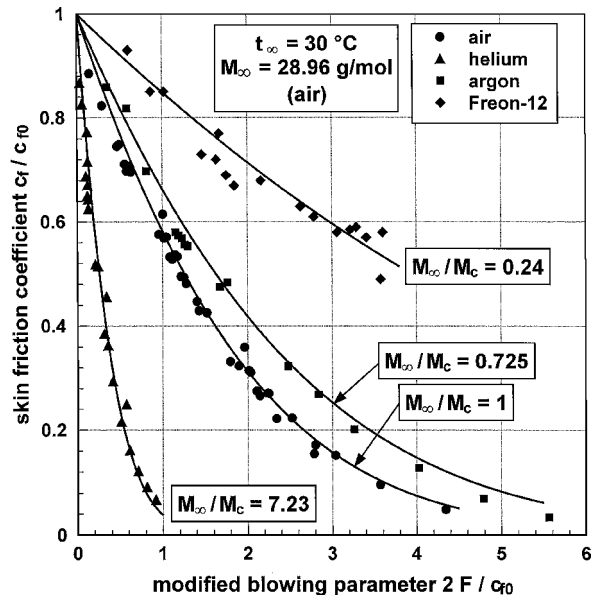

Fig. 3 Decrease of skin friction in the case of isothermal foreign gas transpiration.

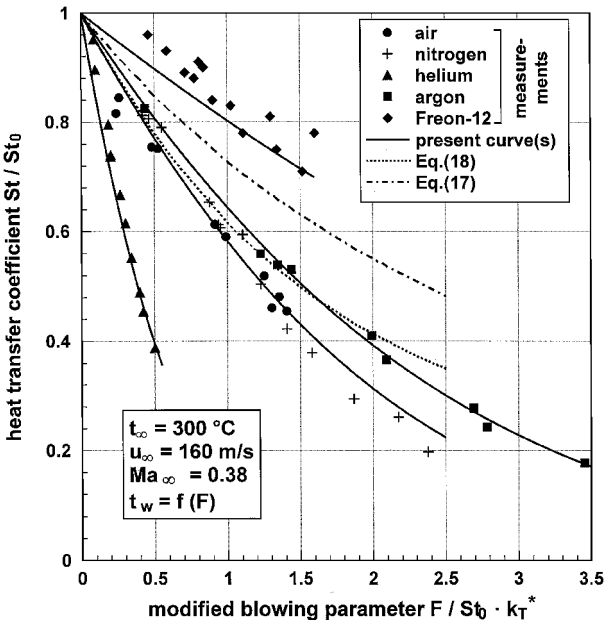

Fig. 4 Decrease of heat transfer due to foreign gas transpiration.

current empirical c_{f0} correlation. The total accuracy of these measurements has to be estimated with approximately 10% because of the nonspecifiable accuracy of the derived laws of the wall (Clauser method).

Decrease of Heat Transfer

A more important problem with respect to practical applications is the decrease of heat transfer due to (foreign) gas transpiration. From the simplified one-dimensional thermal energy balance, a correlation can be derived according to the skin-friction equation (see Kays and Crawford[14]). After adding two new correction factors for property k_M^* and temperature k_T^* influence, this equation becomes

$$\frac{St}{St_0} = \frac{(F/St_0)k_M^* k_T^*}{\exp\left[(F/St_0)k_M^* k_T^*\right] - 1} \tag{16}$$

but with respect to heat transfer, there is only a very small dependence on the temperature ratio in the range of $k_T^* \approx (T_{aw}/T_w)^{0.2,\ldots,0.4}$. In contrast, Fig. 4 shows a considerable effect of cooling gas properties. The best fit property correction factor according to the present test data is given by $k_M^* = (M_\infty/M_c)^{0.6}$. Using Eq. (16), the lines in Fig. 4 were calculated.

Table 2 Comparison of correction factors

Coolant	M_∞/M_c	$c_{pc}/c_{p\infty}$
Helium	7.23	5.17
Nitrogen	≈1	≈1
Argon	0.725	0.51
Freon 12	0.24	0.716

To describe the dependence of Stanton number St/St_0 on the blowing ratio, two empirical correlations taken from other publications[2,4] are compared for the case of air injection. The first correlation is used by Woodruff and Lorenz[2] to describe heat transfer measurements in high-speed flow ($Ma_\infty \leq 8$) on a flat plate (in Fig. 4 assuming $c_{pc}/c_{p\infty} \approx 1$):

$$\frac{St}{St_0} = \frac{c_{pc}}{c_{p\infty}}\frac{F}{St_0} \Bigg/ \left[\left(1 + \frac{1}{3}\frac{c_{pc}}{c_{p\infty}}\frac{F}{St_0}\right)^3 - 1\right] \tag{17}$$

The second equation of Fogaroli and Saydah[4] results from heat transfer measurements on a cone (supersonic flow, air injection):

$$St/St_0 = \sqrt{(F/2St_0)^2 + 1} - F/2St_0 \tag{18}$$

Neither equation is in good agreement with the present test results; there is an additional effect of Mach number obviously, which not could be eliminated by scaling with Stanton number St_0.

Another property correction factor is defined by Kays and Crawford[14] as $k_{cp}^* = (c_{pc}/c_{p\infty})^{0.6}$, an agreement with the present factor k_M^* being only given in the case $c_{pc}/c_{p\infty} = M_\infty/M_c$. A comparison of these terms in Table 2 for the present coolants shows that the k_{cp}^* correction would not give satisfying agreement with the present data. Furthermore, the use of constant molecular weights is more practicable because there is no necessity for a c_p reference temperature discussion.

Modification of the Rannie Equation[10]

An alternative way to estimate the effect of transpiration is to calculate the hot-gas side wall temperature T_w directly using the so-called Rannie equation.[10] When the simplified boundary-layer balances are solved, including the assumptions 1) two-layer-boundary model (viscous sublayer and turbulent layer), 2) convective wall heat flux density $\hat{q}_w$ equal to the increase of specific coolant enthalpy $\rho_w v_w c_{pc}(T_w - T_c)$, and 3) coolant temperature leaving the porous wall T_{cw} equal to the hot-gas side temperature of the wall structure T_w, a dimensionless temperature relation is obtained:

$$\frac{T_w - T_c}{T_\infty - T_c} = \frac{\exp(-\varphi Pr^*)}{1 + (c_{pc}/c_{p\infty})(u_\infty/u_a - 1)[1 - \exp(-\varphi)]} \tag{19}$$

with $\varphi = \rho_w v_w y_a/\eta$ and $Pr^* = \eta_\infty c_{pc}/\lambda_\infty$. Pr^* is a Prandtl number containing properties of different fluids, and subscript a denotes the outer boundary of the viscous sublayer. A detailed development of Eq. (19) is shown in several publications.[10,13] By the differing from the strategy of Rannie,[10] the coordinate y_a and the velocity u_a at the edge of the sublayer are predicted from measurements of the Prandtl coordinates $y_a^+ = u_a^+ = 11.5$ (determination from special laws of the wall) carried out by the present author. Introducing the skin-friction parameter valid for turbulent flat plate boundary layers $c_f/2 = 0.029 Re_x^{-0.2}$, a modified Rannie equation results:

$$\frac{T_w - T_c}{T_\infty - T_c} = \frac{\exp(A\varphi^* Pr^* F)}{1 + (c_{pc}/c_{p\infty})(B\varphi^* - 1)[1 - \exp(A\varphi^* F)]} \tag{20}$$

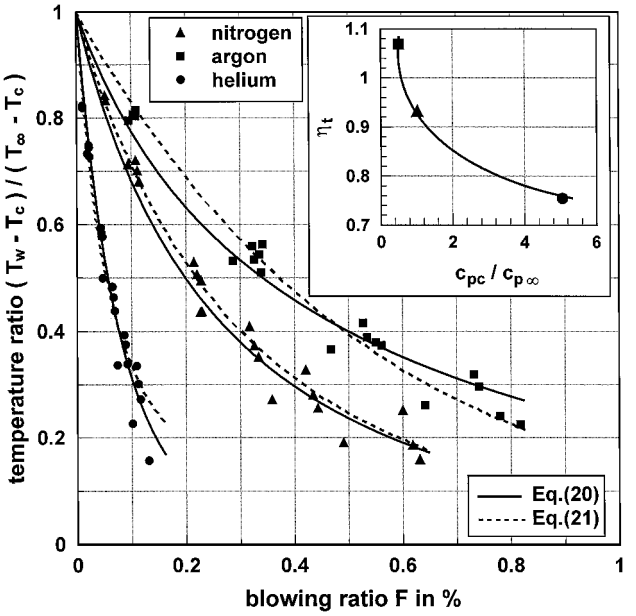

Fig. 5 Measured temperature ratios compared with theory.

with $\varphi^* = \eta_t Re_x^{0.1}$, $A = -67.5$, and $B = 0.51$. The constants, as well as the additional factor η_t, were determined from best-fit investigations using the present experimental results. A further equation is suggested from Laganelli[11] including an arbitrary modification by the present author (term $c_{pc}/c_{p\infty}$ added):

$$\frac{T_w - T_c}{T_\infty - T_c} = \left\{1 + \frac{c_{pc}}{c_{p\infty}} \frac{Re_x^{0.1}}{2.11}\left[\exp\left(57.03 F Re_x^{0.1} Pr^{\frac{2}{3}}\right) - 1\right]\right\}^{-1} \tag{21}$$

Figure 5 shows measurements (symbols) of the temperature difference ratio vs blowing rate F for helium, nitrogen, and argon transpiration, respectively. The lines represent the modified Rannie[10] equation (20), and the inset plots the (best-fit) values for functional dependence of the correcting factor η_t from the heat capacity ratio $c_{pc}/c_{p\infty}$. The broken lines show theoretical results using the arbitrary modified Laganelli[11] correlation Eq. (21). Both curves are in good agreement with the measured temperature ratios.

Critical Blowing Ratio

A well-known phenomenon of turbulent boundary layers is the flow separation. As shown in the last paragraphs, the increase of the blowing ratio F results in decreasing wall shear stress τ_w, but the exponential behavior of Eq. (15) at high blowing ratios does not describe the reality. Essentially, a critical blowing parameter F_{crit} exists that corresponds to the wall shear stress $\tau_w = \eta_w \, du/dy|_w \to 0$ (flow separation).

To investigate the separation of flow due to foreign gas transpiration, a special measuring device was used. A wall shear stress equal to zero is approximately given with zero velocity parallel to the wall at the probe position nearest to the wall $u(y \to 0)$, and this is identical to a zero dynamic pressure. For this reason, the pitot probe was positioned at the wall ($y \approx 0.125$ mm) while increasing the blowing ratio F step by step using different injectants. In this way measuring points $p_{\text{dyn}} = f(F)$ are obtained. To compare different flow and transpiration conditions, the dynamic pressure was scaled using $p_{\text{dyn},0}$ (without blowing) and plotted vs a special modified blowing parameter (Fig. 6).

All test data are in good agreement when using a special property correction factor $k_M^{**} = (M_\infty/M_c)^{0.9}$ and a temperature correction factor $k_T^{**} = (T_{\text{aw}}/T_w)^{0.5}$ (only small influence). The approximating function shows a point of intersection with the x axis at (k_T^{**} neglected)

$$(2F_{\text{crit}}/c_{f0})(M_\infty/M_c)^{0.9} \approx 5.0 \tag{22}$$

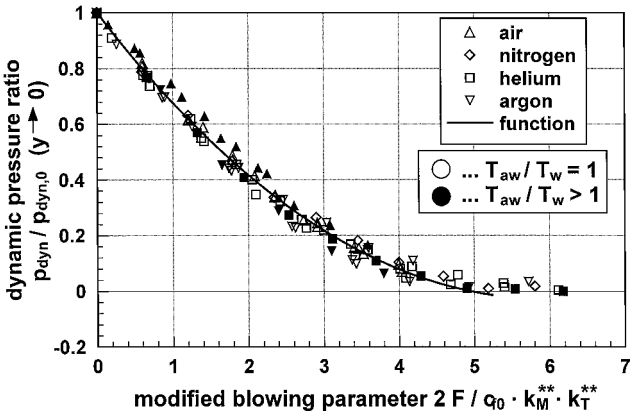

Fig. 6 Measurement of flow separation due to foreign gas transpiration.

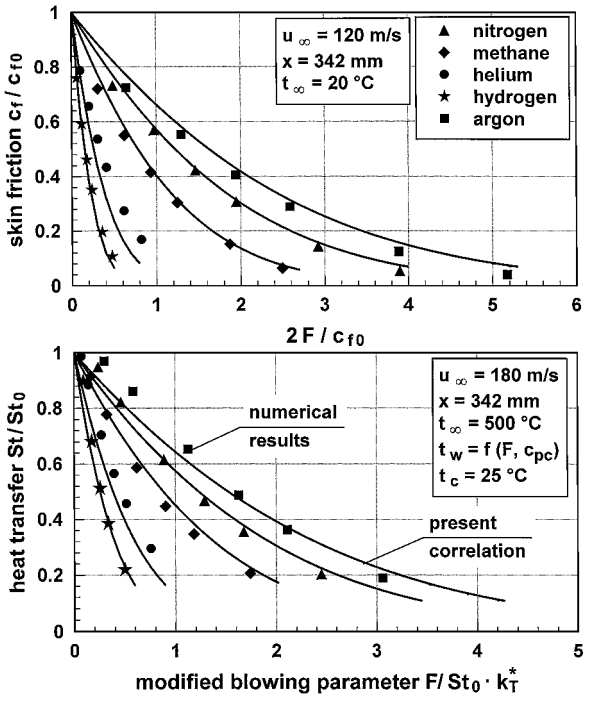

Fig. 7 Comparison of numerical and empirical skin-friction and heat transfer results.

This point indicates flow separation, and the effect of foreign gas properties is excellently accounted for. Many publications dealing with flow separation problems are known; the suggested values of the modified critical blowing parameter are in the range of $3.5 \leq 2F_{\text{crit}}/c_{f0} \leq 6.0$ (different injectants). A survey of several investigations was given by Kutadeladse and Leontiev.[15]

Numerical Investigations

The numerical solution of the turbulent boundary-layer balance equations (mass, momentum, thermal energy, and diffusion) published by Landis[9] was used to carry out skin-friction and heat transfer calculations in the case of foreign gas transpiration. Some of the assumptions included in this procedure are 1) two-dimensional flat plate turbulent boundary layer, 2) use of the mixing length hypothesis of van Driest to describe turbulent viscosity, 3) turbulent Prandtl and Schmidt numbers are constant (selected Prandtl number $Pr_t = 0.87$ and Schmidt number $Sc_t = 0.8$), and 4) discretization using central differences. Some modifications of the original algorithm (for instance, new property routines and modified processing sequence) yield a very good agreement with present experimental skin-friction and heat transfer results. For this reason extensive calculations have been carried out.

Figure 7 shows a selection of skin-friction and heat transfer data comparing numerical (symbols) and empirical results [lines,

Eqs. (15) and (17) including factors k_M and k_M^*]. The agreement is very good using H_2, He, CH_4, N_2, and Ar as blowing gases. Further investigations using heavy gases such as CO_2, SO_2, Freon 12, and Xe give an unsatisfactory or no agreement. However, in this regard it has to be stated that there is also no agreement of numerical Freon 12 results and experimental data[5] (see Figs. 3 and 4). Perhaps the insufficiency of heavy gas calculations has to be traced back to an incorrect determination of the binary gas mixture properties; however, there is no practical application for the use of such gases for transpiration cooling because of their inefficiency.

Combustion Chamber Investigations

Test Facility and Model Combustor

Two facilities are available at DLR, German Aerospace Research Center, in Lampoldshausen for investigations in the field of transpiration cooled combustion devices. For fundamental research, there is the M3 Micro Combustor[3,16] with pressures up to 2 MPa. The P8 is a test facility for research and technology studies in the field of high-pressure liquid oxygen/gaseous hydrogen (LOX/GH_2) rocket combustion devices. The high-pressure combustor in use for the present experiments (see Fig. 8) consists of up to six independent caloric cooled segments with an inner diameter of 50 mm and a length of 50 mm. Although the startup transients last only a few seconds, the typical test duration for the experiments reported varies between 15 and 20 s.

Hot-Gas Conditions

Compared to the operating conditions for the previous experiments at DLR, German Aerospace Research Center, which were performed with the M3 Micro Combustor, the Reynolds numbers which can be achieved with the P8 are about one order of magnitude higher. The combustion chamber pressure can be varied from 4 to 10 MPa keeping the mixture ratio of oxygen and hydrogen constant at $R_{OF} = 6.0$. When chemical equilibrium is assumed, the combustion chamber temperature varies between $3520 \leq T_\infty \leq 3640$ K. Because the operating conditions at the P8 test facility are quite similar to the real rocket engine conditions, one can demonstrate the effectiveness of transpiration cooling at relevant boundary conditions. The hot-gas conditions for a porous segment with 31% porosity are given in Table 3.

Table 3 Hot-gas conditions at P8 test facility[a]

Parameter	Different runs			
T_∞, K	3520	3574	3611	3639
ρ_∞, kg/m^3	1.706	2.537	3.341	4.134
$c_{p\infty}$, kJ/(kg · K)	11.20	10.45	9.96	9.59
$Re_d \times 10^{-5}$	2.78	4.32	5.46	6.92
p_∞, MPa	3.8	5.7	7.6	9.4
$\dot{m}_{O_2}$, kg/s	0.828	1.295	1.765	2.236
$\dot{m}_{H_2}$, kg/s	0.138	0.216	0.294	0.373

[a] $R_{OF} = 6.00$, $Pr_\infty = 0.586$, and pore size 5 μm.

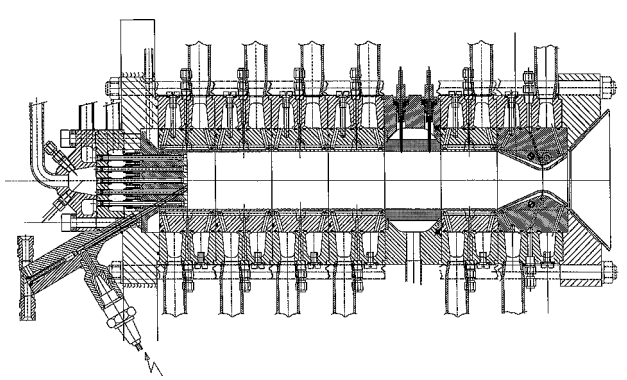

Fig. 8 Modular LOX/GH_2 model combustor B at the P8 test facility at DLR, German Aerospace Research Center, in Lampoldshausen.

Table 4 Coolant conditions at P8 test facility[a]

Parameter	Value
$\dot{m}_c$, kg/s	0.037–0.100
$F \times 10^{-3}$	6.2–26.7
v_c, m/s	1.47–5.28

[a] Transpirant GH_2, $T_c = 300$ K.

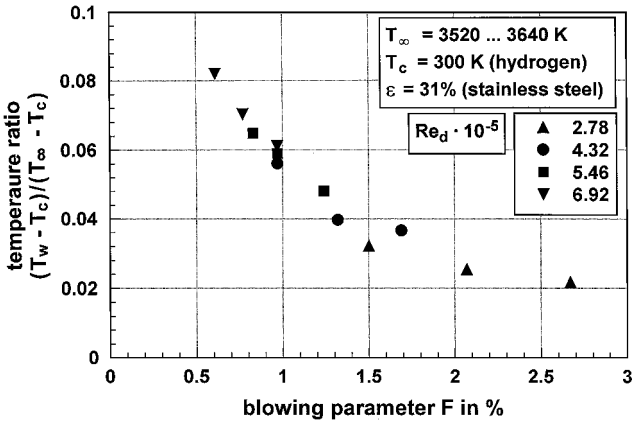

Fig. 9 Test results of transpiration cooled LOX/GH_2 combustion chamber.

Coolant Flow Conditions

Thus far only GH_2 at ambient temperature has been used as transpirant at various mass flow rates. Different mass flow rates can be reached by adjusting the set pressure of the supply system and the diameter of a sonic nozzle in the supply system accordingly. The operating range of the coolant is given in Table 4.

Experimental Results

To check the applicability of empirical results presented, about 25 experiments have been realized. Tests were carried out at various combustion chamber pressures and two different wall porosities of 20 and 31%, respectively. The experimental results for 31% porosity are shown in Fig. 9, where the temperature ratio $(T_w - T_c)/(T_\infty - T_c)$ is plotted vs the blowing ratio F for different Reynolds numbers Re_d. The results may be summarized as follows.

1) For the entire range of Reynolds numbers Re_d and porosities covered experimentally, the temperature ratio increases with decreasing blowing ratio F.

2) Larger Reynolds numbers, which correspond to higher combustion chamber pressures, yield higher temperature ratios.

The decreasing temperature ratio with increasing blowing parameter is a general statement; the influence of the Reynolds number Re_d can be described using a modified equation similar to Eq. (16) including $k_{c_p}^*$ and $k_T^* = 1$ adding a special empirical correction factor.[16]

To compare the combustion chamber test data with the introduced modified empirical correlation Eq. (16), the transformation of temperature ratio data $(T_w - T_c)/(T_\infty - T_c)$ into heat transfer correlations St/St_0 is necessary. For this reason, a simplified energy balance is used, including the assumptions of Rannie[10] (especially $T_{cw} = T_w$):

$$\underbrace{St\rho_\infty u_\infty c_{p\infty}(T_\infty - T_w)}_{\text{convective heat flux}} = \underbrace{\rho_w v_w c_{pc}(T_w - T_c)}_{\text{coolant enthalpy increase}} \tag{23}$$

(hot-gas temperature $T_{aw} \approx T_\infty$). Multiplying Eq. (23) by Stanton number St_0 and rearranging yields an equation to predict St/St_0 depending on the temperature ratio:

$$\frac{St}{St_0} = \frac{F}{St_0}\frac{c_{pc}}{c_{p\infty}}\left(\frac{T_\infty - T_c}{T_w - T_c} - 1\right)^{-1} \tag{24}$$

The Stanton number without transpiration is calculated using an empirical correlation valid for combustion devices[16] including temperature correction.

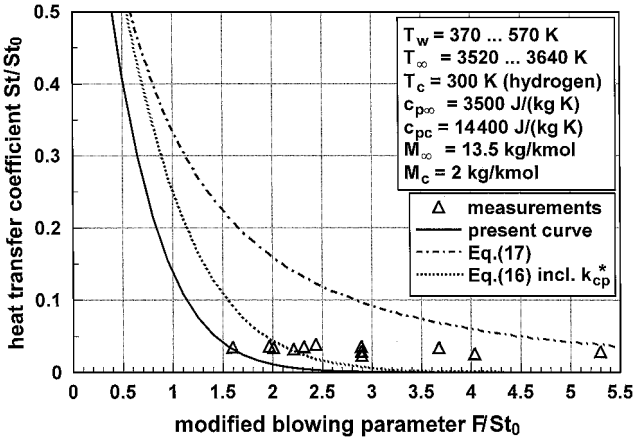

Fig. 10 Transformed heat transfer data of P8 test facility.

Heat transfer data with hydrogen transpiration corresponding to Fig. 9 are shown in Fig. 10. Because of the very strong blowing conditions, the Stanton numbers are only in the range of 4% of unblown reference data. The heat capacity $c_{p\infty}$ is related to a property reference temperature $T_{\text{ref}} = (T_\infty + T_w)/2$ according to the St_0 Stanton number definition. In the case of $c_{p\infty} = f(T_\infty)$, the Stanton numbers increase to approximately 10% of the unblown reference data because of the strong temperature dependence of hot-gas heat capacity $c_{p\infty}$. The experimental results plotted in Fig. 10 show the disappearance of convective heat transfer in the case of flow separation due to high blowing ratios.

After substracting 5% radiative heat transfer due to H_2O vapour radiation (molfraction approximately 60%), the resulting Stanton numbers are equal to zero, which is feasible because Stanton number does not include radiative heat transfer. When the critical blowing criterion Eq. (22) is considered and the Reynolds analogy $c_{f0}/2 = St_0$ is assumed, the present critical (modified) blowing ratio in the case of H_2 transpiration gives $F_{\text{crit}}/St_0 \approx 1$ ($M_\infty/M_c \approx 7$). For this reason there is probably no classical boundary layer but rather a film consisting only of coolant at the wall. The coolant film thickness increases with increasing blowing ratio.

On examination of the plotted empirical results, strong differences are visible. The present correlation [Eq. (16) with k^*_M and $k^*_T = 1$] shows a good agreement because it describes the vanishing of the convective heat transfer. The equation of Kays and Crawford[14] [Eq. (16) with $k^*_{c_p}$ and $k^*_T = 1$] also gives a satisfactory agreement because of $M_\infty/M_c \approx c_{pc}/c_{p\infty}$ in the case of H_2 coolant. The agreement of the Woodruff and Lorenz[2] equation [Eq. (17)] is poor.

Summary

Transpiration of gas through a porous wall into a turbulent boundary layer has a strong influence on boundary-layer characteristics, particularly skin friction, including flow separation and heat transfer. This influence depends primarily on the blowing ratio, as well as the blowing gas properties. Secondary effects are given due to temperature ratio and Reynolds number. It was shown that the impact of coolant properties can largely be taken into account by using the molecular weight ratio M_∞/M_c. In the case of high blowing ratios, the boundary layer separates, and a coolant film probably develops. There is no danger of thermal overheating, but the necessity of such high blowing ratios has to be questioned.

Acknowledgment

The work at the Dresden University of Technology was supported by the German Research Council under Contract Hu 644/1-3.

References

[1]Leadon, B. M., and Scott, C. J., "Transpiration Cooling Experiments in a Turbulent Boundary Layer at M = 3," *Journal of the Aeronautical Sciences*, Vol. 23, No. 8, 1956, pp. 798, 799.

[2]Woodruff, L. W., and Lorenz, G. C., "Hypersonic Turbulent Transpiration Cooling including Downstream Effects," *AIAA Journal*, Vol. 4, No. 6, 1966, pp. 969–975.

[3]Lezuo, M., and Haidn, O. J., "Transpiration Cooling in H2/O2-Combustion Devices," AIAA Paper 96-2581, 1996.

[4]Fogaroli, R. P., and Saydah, A. R., "Turbulent Heat Transfer and Skin-Friction Measurements on a Porous Cone with Air Injection," *AIAA Journal*, Vol. 4, No. 6, 1966, pp. 1116, 1117.

[5]Romanenko, P. N., and Kharchenko, V. N., "The Effect of Transvers Mass Flow on Heat Transfer and Skin Friction Drag in a Turbulent Flow of Compressible Gas along a Arbitrarily Shaped Surface," *International Journal of Heat and Mass Transfer*, Vol. 6, pp. 727–738.

[6]Baronti, P., Fox, H., and Soll, D., "A Survey of the Compressible Turbulent Boundary Layer with Mass Transfer," *Astronautica Acta*, Vol. 13, 1972, pp. 1023–1044.

[7]Ness, N., "Foreign Gas Injection into a Compressible Boundary Layer on a Flat Plate," *Journal of the Aeronautical Sciences*, Vol. 28, No. 8, 1961, pp. 27–40.

[8]Suzuki, K., "A Simple Theory for Heat and Mass Transfer in a Compressible Turbulent Boundary Layer on a Flat Plate with Foreign Gas Transpiration," *Memoirs Faculty Engineering Kyoto University*, Vol. 42, No. 2, 1980, pp. 153–174.

[9]Landis, R. B., "Numerical Solution of Variable Property Turbulent Boundary Layer with Foreign Gas Injection," Ph.D. Dissertation, Univ. of California, 1971.

[10]Rannie, W. D., "A Simplified Theory of Porous Wall Cooling," Jet Propulsion Lab., Progress Rept. 4-50, California Inst. of Technology, Pasadena, CA, 1947.

[11]Laganelli, A. L., "Comparison Between Film Cooling and Transpiration Cooling Systems in High Speed Flow," AIAA Paper 70-153, 1970.

[12]Stevenson, T. N., "A Law of the Wall for Turbulent Boundary Layers with Suction and Injection," College of Aeronautics, Rept. Aero. 166, Cranfield Univ., Cranfield, England, U.K., July 1963.

[13]Meinert, J., "Skin Friction and Heat Transfer in Turbulent Boundary Layers with Foreign Gas Transpiration," Ph.D. Dissertation, Dept. of Mechanical Engineering, Dresden Univ. of Technology, Dresden, Germany, Oct. 2000 (in German).

[14]Kays, W. M., and Crawford, M. E., *Convective Heat and Mass Transfer*, 2nd ed., McGraw–Hill, New York, 1980.

[15]Kutadeladse, S. S., and Leontiev, A. I., *Heat and Mass Transfer and Friction in Turbulent Boundary Layers,* 1st ed., Hemisphere, New York, 1990.

[16]Serbest, E., Haidn, O. J., Hald, H., Korger, G., and Winkelmann, P., "Effusion Cooling in Rocket Combustors Applying Fiber Reinforced Ceramics," AIAA Paper 99-2911, 1999.

T. C. Lin
Associate Editor